Generalized phenomenological models of the yrast band

Dennis Bonatsos and Abraham Klein
Department of Physics, University of Pennsylvania, Philadelphia, Pennsylvania 19104
(Received 3 August 1983)

The variable moment of inertia model has been generalized so as to be applicable to transitional and vibrational nuclei by requiring that the extended models reduce at low angular momentum, J, to the polynomial dependence which agrees with the data. This dictates the introduction of at least three-parameter generalized phenomenological models. Two such models, the generalized variable moment of inertia model and the variable anharmonic vibrator model, are described and then tested against known yrast band data. Except for strongly deformed nuclei, these models substantially improve the agreement with the data.

I. INTRODUCTION

In several recent works[1,2] we pointed out a long-standing puzzle associated with the remarkable success of the variable moment of inertia (VMI) formula[3-5] for the yrast band outside its "natural" domain of application, namely rotational nuclei. We also proposed a generalized model, of which the VMI is a special case. Our confidence in the physical basis of the new model (see below) was reinforced by selected applications. The account which follows results from a full analysis along the new lines of all existing data.

The previous work[1,2] describes as fully as our understanding permits the theoretical basis for the new formulas. We shall not repeat this argument, which generalizes those given much earlier[6,7] to "justify" the VMI formula. Certain physical-mathematical viewpoints cannot be stressed too much, however.

At low angular momentum, the yrast band of strongly deformed nuclei can be described by a power series in $J(J+1)$, where J is the angular momentum. This series diverges at some higher value of J, within the range of physical interest, however, and in general before there has been any band crossing.[8] The problem is to find an *analytic continuation* which sums this series. The original VMI work[3] provided such a recipe based on physical intuition, later substantiated by very general arguments.[6,7]

How then do we generalize the physics so as to describe nonrotational nuclei as well? It is now well established experimentally[9] that we can expect yrast bands in all medium and heavy even nuclei which are not too near closed shells. In order to fit the excitation energies of the lowest lying states we must generalize from the variable $J(J+1)$ to an *arbitrary ratio* of the terms in J and J^2, which for later numerical convenience we choose as the linear combination

$$E(J)\cong aJ+bJ(J-2)\ . \tag{1}$$

Most flexibly we should view these as the first two terms of a series in J which converges for sufficiently small J, but which requires analytical continuation (summation) at higher J below the first band crossing. Thus, we take it as a *boundary condition* on the generalized phenomenology that it should reduce, as $J\to 0$, to Eq. (1). Aside from the purely empirical basis for this requirement, this equation summarizes fully the ground band excitation energies of any limiting symmetry of IBM1, the original version of the interacting boson model.[10] (Naturally then, it also accords with a suitable version of the Bohr-Mottelson model.[11,12]) This boundary condition is not satisfied by the original VMI except for rotational spectra where (b/a) is fixed at the value $(\frac{1}{3})$. We have "explained" in our previous work[1,2] why, nevertheless, the VMI fits so well outside its natural domain. However, as we shall see, the formulas proposed below fit even better.

Given the boundary condition (1) at low angular momentum, the general arguments *do not prescribe* whether, in the higher order terms which are to be summed, one should maintain a fixed ratio between terms of successive order, i.e., treat (1) as the variable or allow a more flexible variation. The most general formula proposed by us for the yrast band,

$$E(J)=\frac{J}{\phi_1(J)}+\frac{J(J-2)}{\phi_2(J)}+\tfrac{1}{2}\sum_{i,j=1}^{2}K_{ij}[\phi_i(J)-\phi_{i0}][\phi_j(J)-\phi_{j0}]\ , \tag{2}$$

has five parameters ϕ_{10}, ϕ_{20}, K_{11}, $K_{12}=K_{21}$, and K_{22}. We view $\phi_1(J)$ and $\phi_2(J)$ as independent generalized scaling variables. *Assuming* two such functions, the theoretical arguments require the harmonic terms of (2) as a minimal structure. In Eq. (2) $\phi_1(J)$ and $\phi_2(J)$ are variational parameters for each J,

$$\left.\frac{\partial E(J)}{\partial\phi_i(J)}\right|_J=0,\quad i=1,2\ . \tag{3}$$

However, to fix five parameters in conjunction with (3), we would have to fit five excitation energies.

In light of these excessive requirements we have chosen initially not to pursue an analysis based on a formula as general as (2), though in light of the results described in this paper, such an analysis may be of future interest. We have instead studied two special cases, each of which contains three rather than five parameters and satisfies the boundary condition (1): (i) The generalized VMI (GVMI) is defined by fixing the ratio of the two scaling functions.

Thus we write

$$E(J)=\frac{J+XJ(J-2)}{\phi(J)}+\tfrac{1}{2}K[\phi(J)-\phi_0]^2 . \quad (4)$$

Since for X fixed at $(\frac{1}{3})$ this becomes the usual VMI, the GVMI should generally improve the fit of the VMI. (ii) We define the variable anharmonic vibrator model (VAVM) by setting $\phi_1(J)$ to be a constant and only allowing $\phi_2(J)$ to vary. Thus we write

$$E(J)=aJ+\frac{J(J-2)}{\theta(J)}+\tfrac{1}{2}C[\theta(J)-\theta_0]^2 . \quad (5)$$

In this case, it is easy to see that $\theta(2)=\theta_0$ and thus $a=[E(2)/2]$. For the near harmonic limit, we expect $(a\theta_0)^{-1}\ll 1$.

Our initial prejudices were certainly in favor of Eq. (4). We were led to consider Eq. (5) only after encountering selected difficulties in the choice of parameters in the analysis based on (4).

After consideration of some elementary properties of each model in Sec. II, in Secs. III and IV, we give a summary of the results of our analysis based on the two models.

II. RANGE OF VALIDITY OF MODELS

This discussion parallels the one carried out in Ref. 3 for the VMI model. First consider the GVMI, Eq. (4). The variational condition $[\partial E/\partial\phi(J)]\,|_J=0$ yields

$$K\phi^2(\phi-\phi_0)=J+XJ(J-2) . \quad (6)$$

One limit of the theory clearly corresponds to letting $K\to\infty$. For (6) to be consistent, we must have $\phi(J)\to\phi_0$ like K^{-1}. This yields the energy formula

$$E(J)=\frac{J+XJ(J-2)}{\phi_0} . \quad (7)$$

One is tempted to consider $K\to 0$ for the other limit. This is incorrect. The other limit is determined by our boundary condition (1). This can be reformulated, for our purposes, by the requirement that $\phi(J)$ be analytic at $J=0$. From (6), with $\phi_0'=(d\phi/dJ)\,|_{J=0}$, we have

$$K\phi_0^2\phi_0'=1-2X . \quad (8)$$

Assuming that the right-hand side does not vanish [$X=(\frac{1}{3})$ corresponds to the strongly deformed limit and probably the largest sensible value of X], $\phi_0'\to\infty$ if *either* $\phi_0=0$ or $K=0$. The experience of phenomenological analysis renders $\phi_0=0$ the relevant condition. With this value of ϕ_0, we have

$$\phi(J)=\{[J+XJ(J-2)]/K\}^{1/3} \quad (9)$$

and

$$E(J)=\tfrac{3}{2}K^{1/3}[J+XJ(J-2)]^{2/3} . \quad (10)$$

From (7) and (10), respectively, we obtain for the range of $R(4)=[E(4)/E(2)]$,

$$R_{\max}(4)=2+4X_{\max}=(\tfrac{10}{3}) , \quad (11)$$

$$R_{\min}(4)=(2+4X_{\min})^{2/3}=(2)^{2/3}=1.59 , \quad (12)$$

having set $X_{\min}=0$. This choice is based on plausibility. In practice the ratio $R(4)$ seldom dips below the value 2.[9]

Applying exactly the same mode of analysis to Eq. (5) of the VAVM, we obtain for $C\to\infty$,

$$E(J)=aJ+J(J-2)/\theta_0 , \quad (13)$$

and for $\theta_0=0$,

$$E(J)=aJ+\tfrac{3}{2}C^{1/3}[J(J-2)]^{2/3} . \quad (14)$$

On physical grounds, we again require the value (11), corresponding to $(a\theta_0)^{-1}\le(\frac{1}{3})$. For the minimum value, we now have

$$R_{\min}(4)=\frac{4a+6C^{1/3}}{2a}\to 2 \quad (15)$$

as $C\to 0$. Thus for the GVMI

$$(2)^{2/3}\le R(4)\le(\tfrac{10}{3}) , \quad (16)$$

whereas for the VAVM

$$2\le R(4)\le\tfrac{10}{3} . \quad (17)$$

In establishing these limits on the validity of the models, we avoid the necessity of having to push the original VMI beyond its legitimate domain of validity. We have based our work on the premise that the value $R_{\min}$, which defines a critical point of the energy curve,[13] represents a natural limit of the model, and that if one encounters nuclei beyond this pale, what is required is a revision of the theory. The physics then requires the introduction of a more elaborate or flexible model.

The limits of validity of the models are equally well ex-

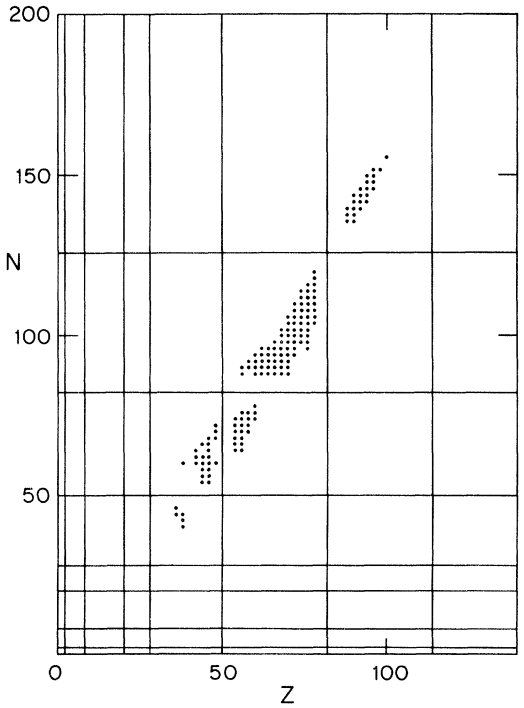

FIG. 1. Even-even nuclides for which yrast bands are known, represented as points on an N vs Z plot. Magic numbers are indicated by solid lines.

TABLE I. Relative accuracy of the three models compared in the text, the VMI, VAVM, and GVMI, for the barium isotopes. DE is the average deviation in energy per energy level tested. n is the number of levels tested.

Nucleus	Z	N	$R_4=E(4)/E(2)$	DE (VMI) (MeV)	DE (VAVM)	DE (GVMI)	n
^{122}Ba	56	66	2.893	0.1031	0.0261	0.0509	3
^{124}Ba		68	2.841	0.1062	0.0164	0.0318	2
^{126}Ba		70	2.777	0.1715	0.0041	0.0182	2
^{128}Ba		72	2.687	0.2439	0.0240	0.0420	3
^{130}Ba		74	2.524	0.0831	0.0004	0.0082	1
^{132}Ba		76	2.428	0.0798	0.0723	0.0601	2
^{144}Ba		88	2.660	0.0567	0.0035	0.0019	1
^{146}Ba		90	2.842	0.0758	0.0433	0.0375	1

pressed in terms of the softness parameter,

$$\text{GVMI: } \sigma_1=(\phi_0'/\phi_0)=(1-2X)/K\phi_0^3 , \tag{18}$$

$$\text{VAVM: } \sigma_2=(\theta_0'/\theta_0)=(-2/C\theta_0^3) , \tag{19}$$

so that (16) and (17) are equivalent to the conditions

$$\infty \geq |\sigma_i| \geq 0, \quad i=1,2 . \tag{20}$$

In relation to the analysis of the results in the next section, we remark that from (7) (the limit $\sigma_1 \rightarrow \infty$) we have

$$X=\frac{R_4-2}{4} . \tag{21}$$

From (13), in the corresponding limit $\sigma_2 \rightarrow \infty$,

$$\frac{1}{a\theta_0}=\frac{R_4-2}{4} . \tag{22}$$

We have also carried out calculations for the original VMI, but shall only report a figure of merit to be compared with corresponding figures of merit for the GVMI and VAVM.

III. COMPARISON OF MODELS

Extensive calculations were done using the GVMI and VAVM models. For the former the three parameters X, K, and ϕ_0 were determined by the values of $E(2)$, $E(4)$, and $E(6)$. For the latter the parameter a was fitted to $E(2)$, whereas $E(4)$ and $E(6)$ determined the values of C and θ_0. A table of the energies obtained from these models for 150 nuclei has been reported elsewhere,[14] together with the values of the parameters which enter the analysis. Comparison is made with the data of Ref. 9 and with calculations made with the original VMI model.

The main aim of the present report is to summarize the results of the calculations (this section) and to illustrate and discuss some systematics of the parameters used in the models (the next section).

In Fig. 1 we show the nuclei studied as points on an N vs Z plot. Of the 150 nuclei analyzed, 19 are vibrational ($2 \leq R_4 \leq 2.4$), 34 fall in transitional region 1 ($2.4 \leq R_4 \leq 2.7$), 21 fall in transitional region 2 ($2.7 \leq R_4 \leq 3$), and 76 are rotational [$3 \leq R_4 \leq (\frac{10}{3})$]. The transition region may include strongly anharmonic, gamma unstable, and weakly deformed nuclei.

In discussing the relative merit of the three models, we chose as a figure of merit the average numerical deviation in energy between experiment and theory. Of the 150 nuclei studied, at least four yrast band energy levels are known for 127 of them: 16 of these are vibrational, 29 lie in transitional region 1, 15 lie in transitional region 2, and 67 are rotational. In general terms, the GVMI gives better results than the original VMI in the rotational and vibrational regions and overwhelmingly better results in the two transitional regions. The VAVM gives even better results than the original VMI in the rotational and vibrational regions and also overwhelmingly better results in the two transition regions. Finally, the VAVM gives

TABLE II. Relative accuracy of the three models compared in the text, the VMI, VAVM, and GVMI, for the erbium isotopes. DE is the average deviation in energy per energy level tested. n is the number of levels tested.

Nucleus	Z	N	$R_4=E(4)/E(2)$	DE (VMI) (MeV)	DE (VAVM)	DE (GVMI)	n
^{156}Er	68	88	2.315	0.0555	0.0150	0.0313	3
^{158}Er		90	3.101	0.0771	0.0168	0.0392	3
^{160}Er		92	3.101	0.0219	0.0160	0.0402	4
^{162}Er		94	3.229	0.0186	0.0126	0.0333	4
^{164}Er		96	3.277	0.0211	0.0200	0.0247	6
^{166}Er		98	3.289	0.0551	0.0179	0.0450	5
^{168}Er		100	3.309	0.0012	0.0043	0.0015	2
^{170}Er		102	3.310	0.0008	0.0023	0.0060	2

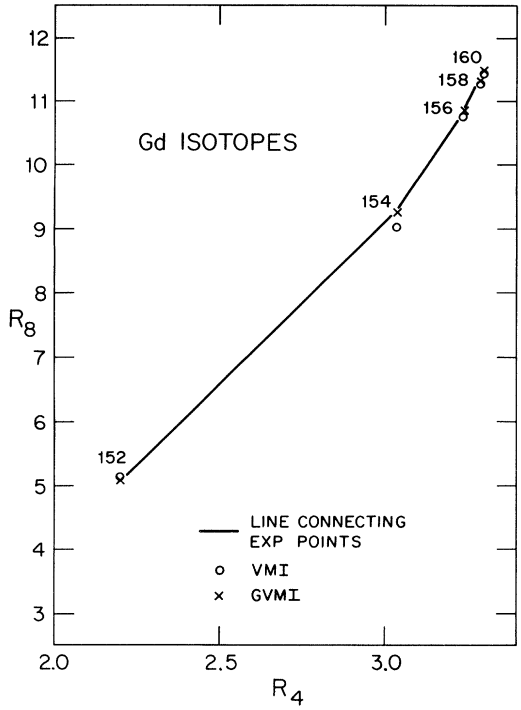

FIG. 2. R_8 vs R_4 for Gd isotopes. Comparison of experiment with VMI and GVMI model calculations, where $R(J)=E(J)/E(2)$ is the ratio of the indicated excitation energies.

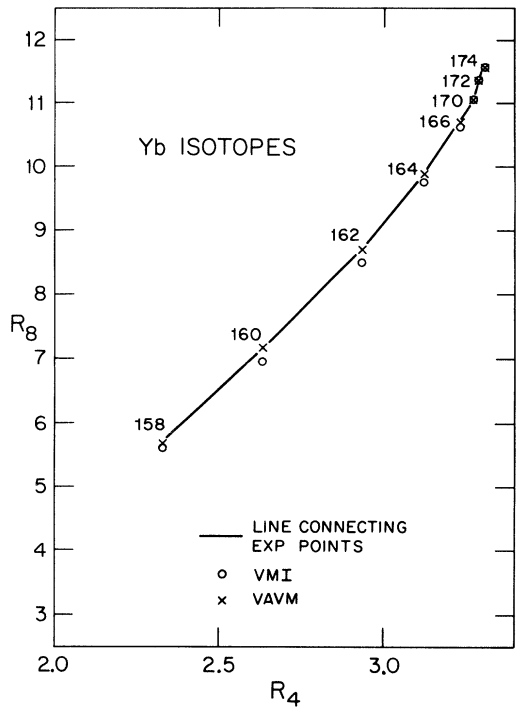

FIG. 4. R_8 vs R_4 for Yb isotopes. Comparison of experiment with VMI and VAVM model calculations.

slightly better results than the GVMI in the rotational region and transitional region 2, but much better results in the vibrational region and transitional region 1.

These general conclusions are illustrated for a set of transitional nuclei (Ba isotopes) in Table I and for a set of largely rotational nuclei (Er isotopes) in Table II. The quantities DE are the figures of merit alluded to above, namely, the numerical deviation between experiment and model per energy level tested. For the barium isotopes the

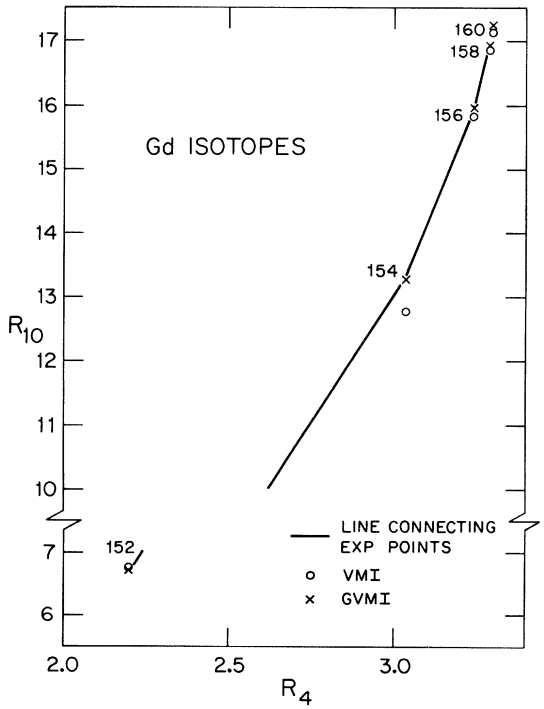

FIG. 3. R_{10} vs R_4 for Gd isotopes. Comparison of experiment with VMI and GVMI model calculations.

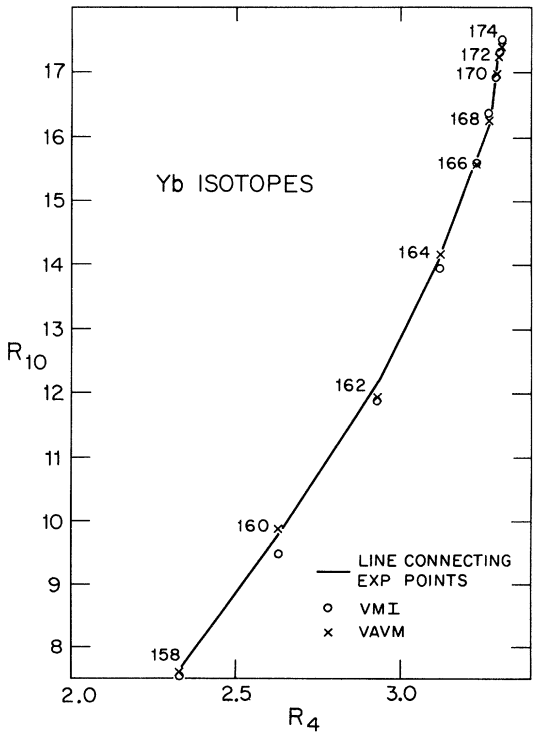

FIG. 5. R_{10} vs R_4 for Yb isotopes. Comparison of experiment with VMI and VAVM model calculations.

TABLE III. Nuclei for which the parameter X of the GVMI model assumed a best fit for $X \geq 0.39$, casting doubt on the GVMI analysis. For every such nucleus there is an acceptable VAVM fit. For other quantities in this table, see Tables I and II.

Nucleus	R_4	DE (VMI)	DE (VAVM)	DE (GVMI)	X	n
$^{80}_{36}$Kr	2.329	0.0666	0.0349	0.0432	0.451	1
$^{98}_{44}$Ru	2.143	0.2088	0.0546	0.0688	0.903	3
$^{100}_{46}$Pd	2.128	0.4689	0.1311	0.0148	2.262	4
$^{102}_{46}$Pd	2.293	0.0960	0.0113	0.0479	0.451	4
$^{106}_{46}$Pd	2.402	0.0787	0.0518	0.0606	0.414	1
$^{108}_{46}$Pd	2.416				0.475	0
$^{110}_{46}$Pd	2.463	0.0124	0.0266	0.0181	0.394	2
$^{112}_{46}$Pd	2.536				0.426	0
$^{108}_{48}$Cd	2.383	0.0286	0.0009	0.0113	0.401	1
$^{116}_{48}$Cd	2.374				0.750	0
$^{148}_{60}$Nd	2.511				0.976	0
$^{150}_{62}$Sm	2.316	0.1417	0.0192	0.0511	0.607	5
$^{188}_{74}$W	3.091				1.573	0
$^{172}_{76}$Os	2.662				0.668	0
$^{174}_{76}$Os	2.741	0.0180	0.0082	0.0042	0.429	1
$^{198}_{78}$Pt	2.419				0.483	1

VAVM is better than the GVMI, which improves upon the VMI, all this *on the average*. For the Er isotopes, the same assertions hold, except for the best rotators, where the VMI seems to be optimal.

The same points are illustrated in a different way in Figs. 2 and 3, where we have plotted R_8 and R_{10}, respectively, vs R_4, where $R_J=[E(J)/E(2)]$ for the known Gd isotopes. Here we compare the experimental results (connected by lines), the VMI results, and the GVMI results. (We have omitted the VAVM results to avoid confusion.) These figures again illustrate the general point that the improvement of the GVMI over the VMI is most substantial in the transition region. Similarly in Figs. 4 and 5, we have plotted R_8 and R_{10} vs R_4 for the Yb isotopes, this time substituting VAVM results for GVMI results. Qualitatively the same remarks apply as for the Gd isotopes.

It emerges from the analysis that the parameter X of the GVMI remains very close to $\frac{1}{3}$ for rotational nuclei (which means that the VMI is nearly optimal in this region as remarked) but exhibits gradually lower values in transitional regions 2 and 1 and the vibrational region, giving generally better results than the original VMI, as stated. This means that the $J(J+1)$ dependence of the rotational term is justified only for rotational nuclei and it is favorable to use the more general form $J+XJ(J-2)$ in the other regions. This is in agreement with the fact that the $J(J+1)$ dependence has been justified theoretically for low J only in the rotational region. The fact that the VAVM gives in general better results than the GVMI, especially in the vibrational region and transitional region 1, means that a better description is achieved by allowing separate scaling variables for J and $J(J-2)$, as is done in Eq. (2), even in the case where we restrict one of these scaling variables to be constant, as in the case of the VAVM. It is thus expected that the five-parameter formula of Eq. (2) can give much more accurate results. A four-parameter model can also be obtained by allowing $K_{12}=K_{21}=0$.

Although the bulk of the solutions followed qualitative physical expectations, we obtained GVMI solutions for 16 nuclei with $X \geq 0.39$. The nuclei in question and the X values are listed in Table III. It should be remarked that for these nuclei, experimental results up to $J=8$ are known for only 9 of them. In general, the GVMI gives results better than the VMI but worse than the VAVM. Only for ^{100}Pd and ^{174}Os does the GVMI give the best results. We tend to believe that these solutions are numerically acceptable, but lack a clear physical significance be-

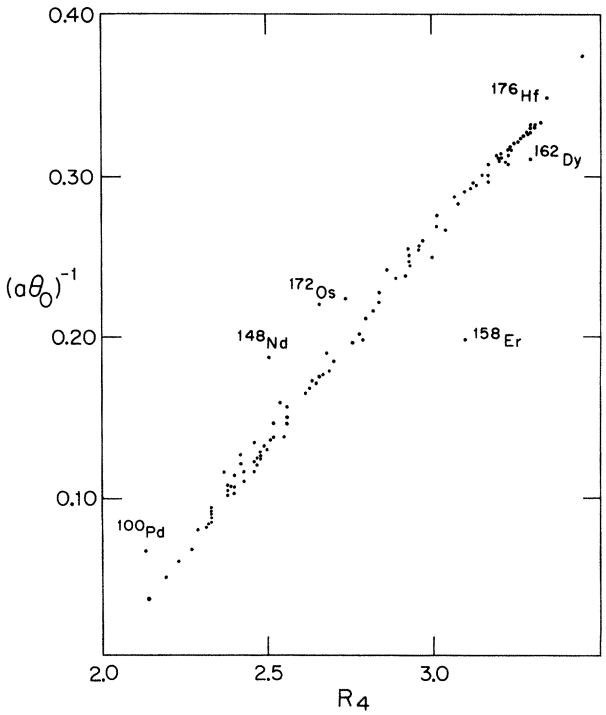

FIG. 6. The VAVM parameter combination $(a\theta_0)^{-1}$ vs R_4, illustrating the remarkable agreement with Eq. (22).

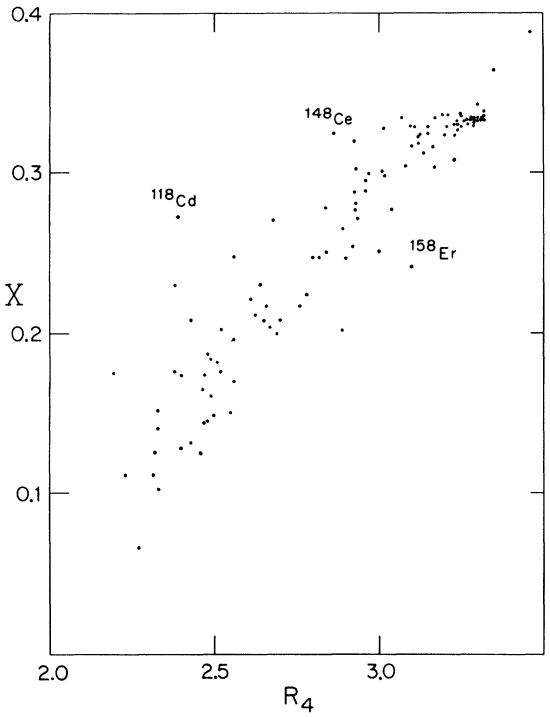

FIG. 7. The GVMI parameter X vs R_4, illustrating the rough correlation with Eq. (21).

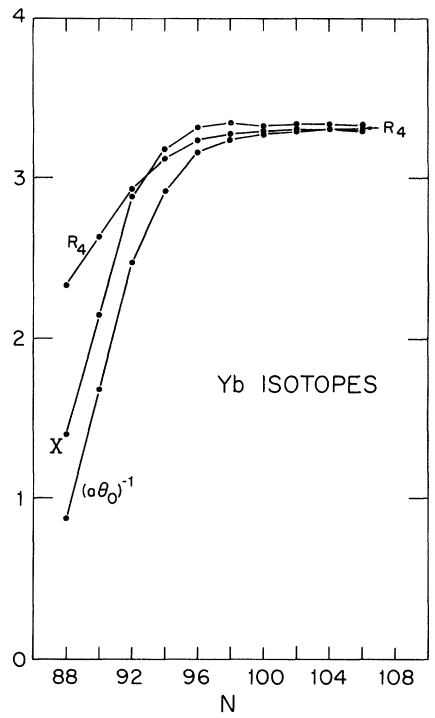

FIG. 8. The VAVM parameter combination $(a\theta_0)^{-1}$, the GVMI parameter X, and R_4 vs N for the Yb isotopes, illustrating similar smooth behavior.

cause they correspond mostly to values outside the accepted domain of validity. Especially for ^{100}Pd, the solution obtained is of much better quality than the VMI or VAVM solutions, but has the highest X obtained (2.262). This may be related to the fact that ^{100}Pd is the only pseudomagic nucleus studied here.[15]

IV. PARAMETER SYSTEMATICS

Turning now to systematics of the parameter sets, in Fig. 6 the quantity $(1/a\theta_0)$ of the VAVM vs R_4 is shown. There is a remarkable correlation with the limiting straight line (22), all points lying on or slightly above, giving $1/(a\theta_0)=\frac{1}{3}$ for $R_4=\frac{10}{3}$ and $1/(a\theta_0)=0$ for $R_4=2$. Only ^{188}W gives a value of $1/(a\theta_0)$ significantly larger than $\frac{1}{3}$ (0.604), which is not shown in the figure.

A similar graph of the parameter X of the GVMI vs R_4 is given in Fig. 7. Again most points are close to or slightly above the line $X=(R_4-2)/4$, given in Eq. (21), although the correlation is not as good as in Fig. 6. Sixteen nuclei with $X\geq 0.39$ fall far from this line and are not shown (see Table III). Six of them are Pd isotopes. The remaining ten have the common characteristic of exhibiting a lower R_4 than all the neighboring nuclei of the same element studied here (i.e., for which good results were obtained). Nine of them fall between $X=\frac{1}{3}$ (the standard VMI value) and $X=\frac{1}{2}$, and the remaining six exceed this value. Seven of these nuclei are "vibrational" (^{80}Kr, ^{98}Ru, ^{100}Pd, ^{102}Pd, ^{108}Cd, ^{166}Cd, and ^{150}Sm), and seven more lie in transitional region 1 (^{106}Pd, ^{108}Pd, ^{110}Pd, ^{112}Pd, ^{148}Nd, ^{172}Os, and ^{198}Pt). Only one is rotational (^{188}W) and one lies in transitional region 2 (^{174}Os). This behavior can be explained by using the result found above in the $\sigma_1\to 0$ limit, namely that $X_{\min}=(R_4-2)/4$. What happens is clear: The values of X follow more or less the value of R_4. If good agreement with the experimental results is obtained for $\frac{1}{3}\geq X\geq X_{\min}$, a point close to or

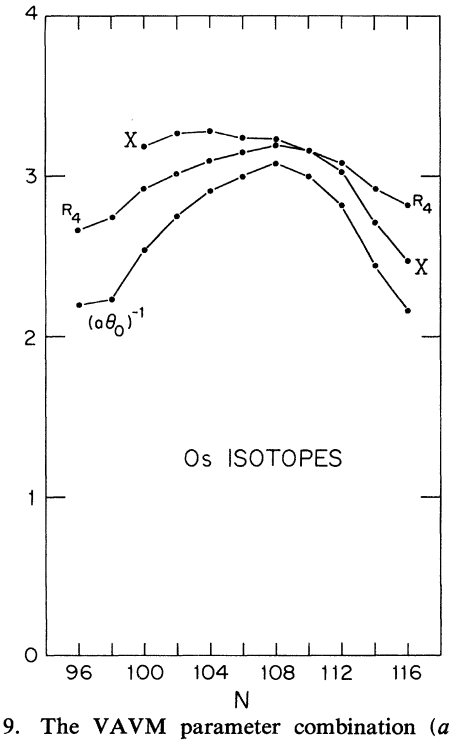

FIG. 9. The VAVM parameter combination $(a\theta_0)^{-1}$, the GVMI parameter X, and R_4 vs N for the Os isotopes, illustrating similar smooth behavior.

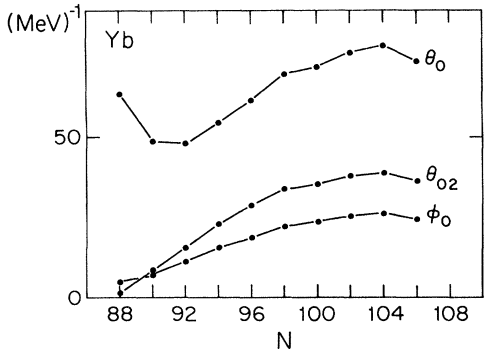

FIG. 10. The VAVM parameter θ_0 and the GVMI parameter ϕ_0 vs N for the Yb isotopes, illustrating similar smooth behavior.

above the line $X=(R_4-2)/4$ appears in Fig. 7. As R_4 decreases, so does X. But X cannot become lower than $X_{\min}$. If $X_{\min}$ is reached with no good agreement obtained, X jumps up to high values, higher than $\frac{1}{3}$.

The quantity $1/(a\theta_0)$ of the VAVM and the parameter X of the GVMI behave exactly like R_4 as functions of N for a given Z, i.e., they increase when R_4 increases and decrease when R_4 decreases. This includes bendings at $N=68$ for Xe, at $N=104$ for Yb and Pt, at $N=108$ for Hf, W, and Os, and at $N=142$ for Th. In Figs. 8 and 9 the quantities R_4, $1/(a\theta_0)$, and X are given as functions of N for Yb and Os, respectively. The features mentioned above (similar smooth behavior, bendings at $N=104$ and $N=108$) can be observed.

The ground state moment of inertia parameters, θ_0 of the VAVM and ϕ_0 of the GVMI, also behave in general like R_4 as functions of N for a given Z, i.e., they increase when R_4 increases and decrease when R_4 decreases in each region. Bending occurs at $N=104$ for Yb, Hf, and Pt and at $N=108$ for W and Os, as previously remarked in Ref. 3. However, the correlation is not as clear as that discussed in the preceding paragraph, with a number of exceptions found. Some nuclei with $N=88$ (^{144}Ba, ^{150}Sm, ^{152}Gd, ^{154}Dy, ^{156}Er, and ^{158}Yb) exhibit θ_0 values much higher than their neighboring $N=90$ nuclei, although lower values are expected. Φ_0 behaves "properly." Also bending is observed for Th at $N=142$. In Figs. 10 and 11

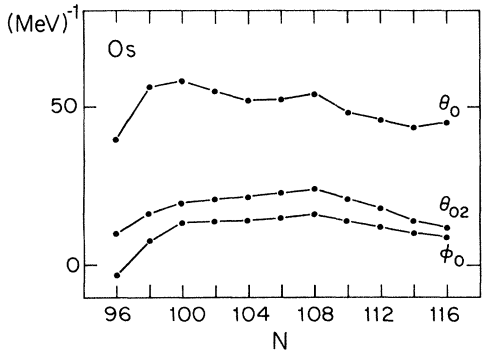

FIG. 11. The VAVM parameter θ_0 and the GVMI parameter ϕ_0 vs N for the Os isotopes, illustrating similar smooth behavior.

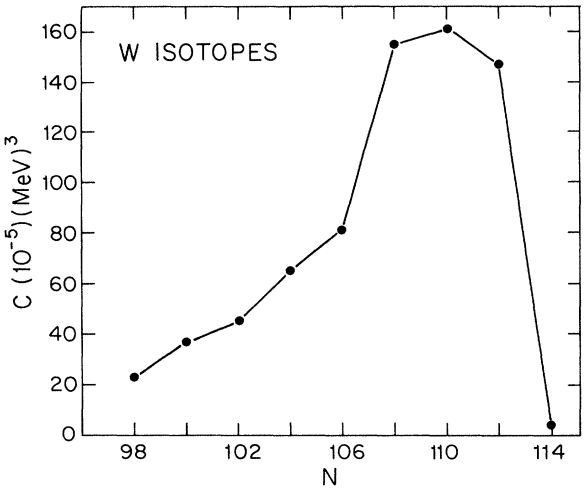

FIG. 12. The "restoring force" constant C of the VAVM model vs N for the W isotopes. According to Eq. (19) of the text this is equivalent to a plot of the reciprocal of the softness parameter.

the parameters θ_{02}, θ_0, and Φ_0 are given as functions of N for Yb and Os. Here θ_{02} corresponds to the moment of inertia parameter of Ref. 3 [$=\frac{2}{3}\phi_0(X=\frac{1}{3})$]. The bendings at $N=104$ and $N=108$, respectively, as well as the special behavior of θ_0 for ^{158}Yb, can be observed. Among other quantative features are the following: θ_0 and ϕ_0 exhibit their highest values in Ra and the actinides. θ_0 is also very high for ^{152}Gd and ^{154}Dy (both are vibrational nuclei with $N=88$). θ_0 becomes negative for $R_4\leq 2$. No such nucleus was studied here. ϕ_0 becomes negative[16] for $R_4\leq(2+4X)^{2/3}$. This happens for 11 nuclei, all of them having $X\geq 0.39$. The remaining 5 nuclei having $X\geq 0.39$ exhibit low ϕ_0 values.

We turn to the parameters C of the VAVM and K of the GVMI, the so-called restoring forces constants (a misnomer). The systematics of these parameters appears to be more complicated than the behavior of the ground state moment of inertia, usually increasing, however, with

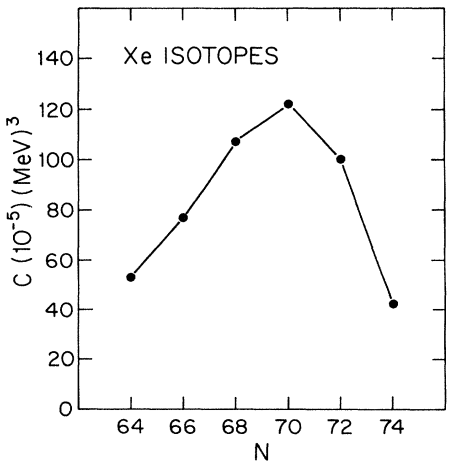

FIG. 13. The "restoring force" constant C of the VAVM model vs N for the Xe isotopes.

R_4. The increase with R_4 appears most decisive for rotational nuclei, where the limits C and $K \to \infty$ encompass the cases of rigid rotation. This correlation, not quite perfect, is illustrated for the parameter C in Fig. 12 for the W isotopes, $A=172-188$. The behavior of K is similar. The sharp change from ^{186}W to ^{188}W may be indicative of a "phase transition." The especially low values of ^{148}Nd, ^{150}Sm, and ^{154}Dy ($N=88$) may have a similar explanation. Figure 13 illustrates that the same correlation is not confined to rotational nuclei. The special behavior observed at $N=68$, 88, 104, 108, and 142 and the lack of backbending at $N=98$ can be attributed to the neutron sublevels of the shell model completed at $N=70$, 90, 104, 110, and 142 and $N=100$ correspondingly.

V. CONCLUSION

The most important conclusion of this work is that the $J(J+1)$ dependence in the VMI formula is exactly valid only in the rotational region. Even with the more general form $J+XJ(J-2)$ giving improved results, there is evidence that a better description is obtained by allowing different scaling factors for J and $J(J-2)$, as done in the VAVM. It is also remarkable that with the range of validity of the original VMI, $2.23 \leq R_4 \leq 10/3$, the VAVM describes nuclei with $R_4 \geq 2$, and the GVMI can in principle describe nuclei with $R_4 \geq 1.59$.

It is probably of interest to investigate the general form suggested in Eq. (2), not for predictive purposes, but rather, by accepting the theoretical structure to determine the J dependence of the scaling functions. Beyond that is the purely theoretical question of why we need two scaling functions in general, when one will do in the rotational region. It is almost certainly of interest to consider the application of our suggestions to band crossing outside the strictly rotational domain.

Finally we wish to emphasize that our work is in no way intended to diminish the theoretical and practical importance of the VMI model, but is rather intended to refine it outside what we consider its natural domain of validity. Concerning this point, however, there is a difference of philosophy between our work and that of Ref. 16, for example.

ACKNOWLEDGMENTS

We are indebted to Dr. G. Scharff-Goldhaber for helpful suggestions and provocative comments. This work was supported in part by the Department of Energy under contract No. EY-76-C-02-3071.

[1]A. Klein, Nucl. Phys. A347, 3 (1980).
[2]A. Klein, Phys. Lett. 93B, 1 (1980).
[3]M. A. J. Mariscotti, G. Scharff-Goldhaber, and B. Buck, Phys. Rev. 178, 1864 (1969).
[4]For a review, see G. Scharff-Goldhaber, C. B. Dover, and A. L. Goodman, Annu. Rev. Nucl. Sci. 26, 239 (1976).
[5]S. M. Harris, Phys. Rev. 138, B509 (1965).
[6]T. K. Das, R. M. Dreizler, and A. Klein, Phys. Lett. 34B, 235 (1971).
[7]A. B. Volkov, Phys. Lett. 35B, 299 (1971).
[8]For a review, see R. M. Lieder, Nucl. Phys. A347, 69 (1980).
[9]M. Sakai, *Quasi Bands* (Institute for Nuclear Study, University of Tokyo, Tokyo, 1982).
[10]*Interacting Bosons in Nuclear Physics,* edited by F. Iachello (Plenum, New York, 1979).
[11]D. Janssen, R. V. Jolos, and F. Dönau, Nucl. Phys. A224, 93 (1974).
[12]A. Klein, C. T. Li, T. D. Cohen, and M. Vallieres, in *Progress in Particle and Nuclear Physics* (Pergamon, Oxford, 1983), Vol. 9, p. 183.
[13]G. Scharff-Goldhaber and M. Dresden, Trans. N.Y. Acad. Sci. 40, 166 (1980).
[14]D. Bonatsos and A. Klein, University of Pennsylvania Report UPR-0217T, 1983.
[15]G. Scharff-Goldhaber, J. Phys. G 5, L207 (1979); Corrigenda 6, 413 (1980).
[16]G. Scharff-Goldhaber and A. S. Goldhaber, Phys. Rev. Lett. 24, 1349 (1970).